Quantum Dots

DOI: 10.1002/anie.200800409

Facile and Rapid One-Step Mass Preparation of Quantum-Dot Barcodes**

*Sébastien Fournier-Bidoz, Travis L. Jennings, Jesse M. Klostranec, Winnie Fung, Alex Rhee, David Li, and Warren C. W. Chan**

Since their creation in 1949 by Woodland and Silver for grocery and warehouse inventory,[1] the broad application and utility of barcodes has continuously expanded. Today, in response to the demand for high-throughput multiplexed detection for elucidation of biomolecular mechanisms and to advancing personalized molecular diagnostics and therapeutics, molecular barcodes are much needed for inventorying biological molecules.[2–4]

Within the context of molecular barcoding, two platforms capable of fulfilling the needs for code recognition and multiplexed detection exist: graphical barcodes utilizing structural recognition and spectroscopic barcodes using the unique optical properties of an embedded material.[2] Whereas each platform maintains the potential to construct large barcode libraries, limitations in barcode stability, reproducibility, or readout impose serious limitations. Graphical barcodes,[5–11] such as etched polymeric or striped metallic structures, suffer a multitude of problems from the complex instrumentation required for both synthesis and readout, the slow data collection rate (approximately 3 Hz for recent polymeric structures[11] compared to several kilohertz detection of microbeads by flow cytometry), to the unstable dispersion of these structures in buffer or media, making them unfit for mainstream applications. While spectroscopic barcodes employ a colorimetric readout, fluorescence-based barcodes are rapidly detected using flow cytometry[12,13] or miniaturized home-built systems.[14] Raman barcodes still require planar array readout after lengthy detection protocols.[15] From a time-efficiency and sensitivity standpoint, fluorescence-based microbead barcodes are therefore best suited for applications in high-throughput multiplexed detection.

[*] Dr. S. Fournier-Bidoz, Dr. T. L. Jennings, J. M. Klostranec, W. Fung, A. Rhee, D. Li, Prof. W. C. W. Chan
Institute of Biomaterials & Biomedical Engineering &
Terrence Donnelly Center for Cellular and Biomolecular Research
Univeristy of Toronto
160 College street, 4th floor, Toronto, ON, M5S 3G9 (Canada)
Fax: (+1) 416-978-4317
E-mail: warren.chan@utoronto.ca
Homepage: http://inbs.med.utoronto.ca

[**] We thank Doug Holmyard for making a cross-section of a CCFF barcode sample for TEM imaging. We thank Dr. Betty Kim for discussion. This project was funded by Genome Canada through the Ontario Genome Institute, and Ministry of Research and Innovation's Ontario Research Fund. J.K. Acknowledges NSERC for a student fellowship.

Supporting information for this article is available on the WWW under http://dx.doi.org/10.1002/anie.200800409.

Fluorescent quantum dots (QDs) boast narrow Gaussian emission line shapes, resistance to photobleaching, high quantum yields, and single-wavelength excitation, whereas molecular dyes suffer from both photobleaching and red-tailed emission;[16,17] thus, QDs are ideal fluorophores for barcoding. However, the construction of QD barcodes has shown minimal advance since their conception in 2001[18] because of difficulties encountered in the mass production of robust and reproducible barcoded materials. Current methods to prepare QD barcodes include the "swelling" technique,[18] QD entrapment inside layer-by-layer charged polymer coatings[19] or mesoporous silica microbeads,[20] and polymerizable QD encapsulation.[21,22] Microbead "swelling" and layer-by-layer techniques result only in surface-level loading of QDs into the polymer,[18,23] which are thus exposed to pH values and environmental factors that destabilize their fluorescence intensity.[24,25] Stability of the barcode (fluorescence profile) requires that the QDs be positioned well within the polymer matrix and do not leak from the bead, and thus, techniques to encapsulate the QDs during the polymerization step were developed.[21,22] However, this process is lengthy, requires considerable presynthetic QD surface modification, and yet results in broadly dispersed microbead sizes. Moreover, a number of these barcode systems (e.g. mesosilica microbeads) do not lend themselves to use for bioassays owing to their high degree of nonspecific binding. We have overcome these problems by creating the concentration-controlled flow-focusing (CCFF) technique.

The process comprises two parts: 1) a pressurizable vessel with variable input/output flows to control any volume change and solution concentration in real time and 2) a nozzle immersed in the vessel for the barcode manufacturing. Figure 1a shows a complete view of the CCFF process as well as an enlarged cross-sectional view of the nozzle. The nozzle accepts inputs from two fluid sources, an organic QD/polymer-containing phase and an aqueous focusing phase, that intersect in the nozzle outlet. Control of the flow rates at both inputs results in the periodic axisymmetric breakup of the fluid stream caused by microfluidic instabilities.[26,27] The result is a steady flow rate that is "pinched off" at a stable frequency of about 160 kHz, forming microbeads of identical volume containing chloroform, polymer, and QDs in exact ratios, therefore generating robust barcodes (see Movie S1 in the Supporting Information). The total volume of fluid generated per hour corresponds to a concentration of about 3×10^6 beads mL^{-1}. The chloroform used to solvate QDs and polymer diffuses into the aqueous phase (solubility = 8.0 mg mL^{-1}), thus casting the polymer into a solidified, homogeneously-dispersed QD barcode. The selection of the

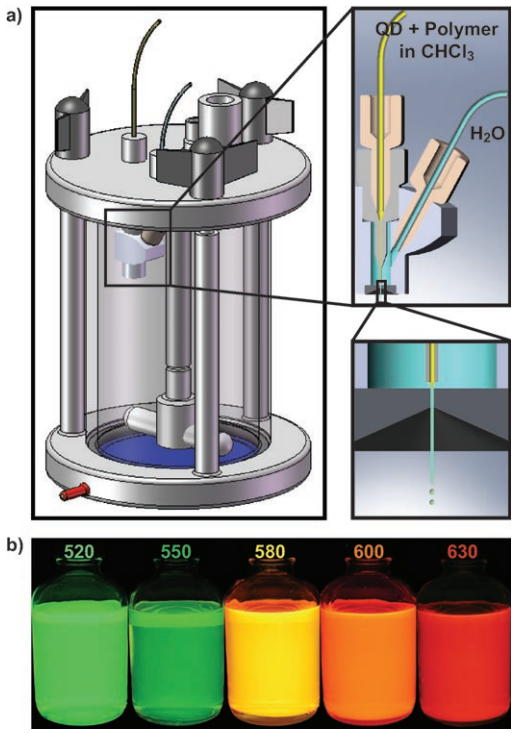

Figure 1. Summary of CCFF barcode presentation. a) Representation of the CCFF process including the concentration reactor and the production nozzle. An enlargement is shown in the top right corner with a cross-sectional diagram of the working flow-focusing nozzle in which a quantum dot fluorophore solution in chloroform with 4% dissolved polymer is introduced through the top line (yellow). The flow-focusing fluid (deionized water) is introduced from the right (blue). A close-up view of the quantum-dot–polymer solution being focused and "pinched off " into microscopic droplets by the water flow is shown on the bottom right corner. Each small droplet formed is an active polymer microbead with homogeneous quantum dot encoding. b) UV-illuminated picture of the five stock solutions of quantum dots used to generate a 105-barcode library. The number printed on each bottle represents the fluorescence emission wavelength in nanometers of the respective quantum dots.

polymer is key to producing QD barcodes. It must be initially organically soluble and then transition into a charged hydrophilic surface after microbead formation. Poly(styrene-*co*-maleic anhydride) was selected, as it serves the purpose of forming both the shell and filler for the microbead, thus protecting the QDs from environmental effects and also providing anhydride functional groups, each of which will hydrolyze to form two carboxylic acid groups when in contact with water. The carboxylates impart anionic charge for solution-based stability and prevention of aggregation, and they permit covalent linkage to biorecognition molecules. A nozzle-only system can only generate a small (subgram) quantity of barcodes owing to the generation of an unmanageable volume of liquid during the process. In contrast, our CCFF process contains a filter (blue in Figure 1a) and valve system (red in Figure 1a) that allows the removal and recycling of water, keeping the volume in the reactor constant while the preparation process continues and preventing the escape of the barcodes from the reaction vessel.

The encoding of a microbead only requires the preparation of an organic solution containing the correct concentration and ratio of different color-emitting QDs (Figure 1b). Figure 2a demonstrates individual images of over 100 unique barcodes from five different QD wavelengths (Figure 1b) using single (bottom), two (middle), or three (top) QD fluorescence wavelengths in a single bead. A maximum of three different levels of intensities were used in the process: 1, 2, and 4. We have devised a shorthand nomenclature when referring to these barcodes that takes into account both wavelength and intensities. The shorthand uses the tens digit of the wavelength and its relative intensity such that 283:142 refers to a barcode containing 5**2**0, 5**8**0, and 6**3**0 nm QDs at relative QD intensity levels of 1, 4, and 2, respectively. Using three colors from a set of five, at three intensity ratios, we generated 60 individual QD barcodes by varying intensity ratios in this pattern: 121, 124, 141, 142, 241, and 421. Similarly, 40 unique barcodes were synthesized using only two QD colors per microbead, and all five single-color QD barcodes were synthesized to finish the set. To further demonstrate that there is no limitation to the number of colors that can be incorporated into a single barcode using this method, a five-color barcode was produced with no added complexity using the entire set of QDs available in this study (see Figure S1 in the Supporting Information). The limit to the possible number of colors per barcode is therefore only dictated by the quality of the QDs used, the width of the fluorescence emission peaks, and the quality of the algorithm used to detect them accurately.

The corresponding emission spectrum for each barcode is presented in Figure 2b for the three-color, two-color, and single-color barcodes. The spectral profile of the bead defines the barcode, and the mixing of QD colors and intensities provides 105 spectrally distinct barcodes. To control relative QD intensities for barcoding, we utilized the relative solution-based QD intensities prior to microbead formation. The final fluorescence spectra of microbeads are different from those in solution (see Figure S2 in the Supporting Information) because of the microbead solidification process, during which a significant shrinking occurs from the loss of organic solvent to the water bath, thus confining QDs into a smaller volume (ca. 27 times, see the Supporting Information). Distance-dependent optical effects such as Förster resonance energy transfer (FRET) or photon reabsorption will occur in this reduced volume, which causes the change in the final relative intensity levels of the QDs emission. Despite such effects, the final barcode has a unique and recognizable signature that can be identified with a deconvolution algorithm that takes into account the relative QD concentration for each color, the photoluminescence overlapped with QD absorption profiles, photoluminescence quantum yields, and the microbead volume.[25] The most critical property of a spectroscopic barcode, however, is its robustness against changing external environments.

The major shortcoming of QD spectroscopic barcodes to date has been their unpredictably variable spectroscopic properties after exposure to sonication, changing pH values and temperatures, or chemical environments.[20,25,28] This variability would prohibit the correct identification of the

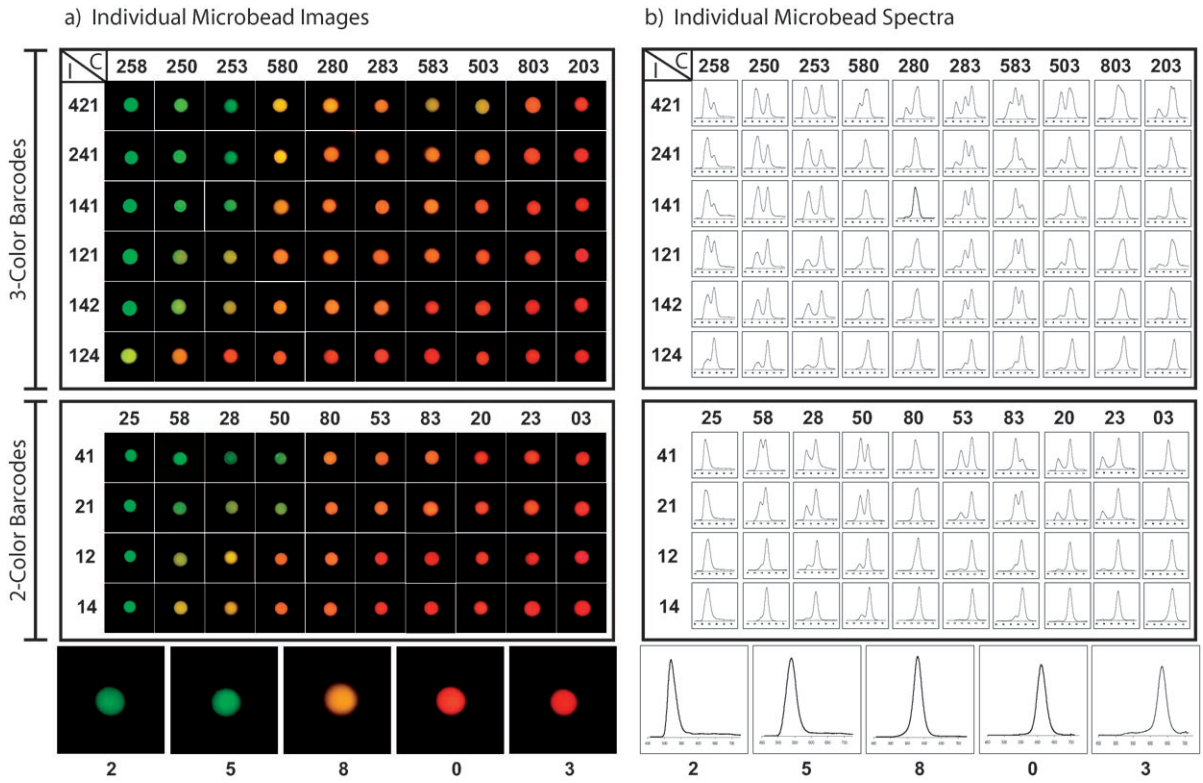

Figure 2. 105-barcode library. a) Microscope images of single 5-μm QD barcodes containing single (bottom), two (middle) and three-color encoding at a variety of relative intensities. The intensities (I) are listed on the left-hand side, and the different wavelength colors (C) are listed along the top for each barcode. b) Corresponding photoluminescence spectra for individual beads are measured as the "fingerprint" for each barcode.

barcodes after their use in biological assays. To compare and test barcode stability, photoluminescence intensity profiles were monitored against the entire range of pH values (pH 0–14), high temperatures up to 95 °C (just below the glass transition temperature of pure polystyrene at 95 °C), and a variety of different chemical environments known to affect QD fluorescence efficiencies. We found that the barcodes synthesized using the present technique were stable to every perturbation that we attempted, where a side-by-side comparison to other encoding techniques resulted in drastic differences (see Table 1, and Figures S3–S8 in the Supporting Information). This could be because the QDs are not just

Table 1: Summary of side-by-side QD barcode comparison study.

	Swelling[a]	Polymer[b]	CCFF
Synthetic steps	3 or more	2	1
Ease of barcoding	difficult	easy	easy
Purification steps	tedious	tedious	not needed
Bead monodispersity	excellent (<3%)	poor (>10000%)	good (<10%)
Workable size range	100 nm–10 μm	undefined	4–20 μm
Buffer stability	poor	good	good
pH stability	6–12	0–14	0–10
Heat stability	54%	87%	88%
Stability to leakage	40%	93%	88%
Bioconjugation	feasible	feasible	feasible
Pros for bioapplications	● very monodisperse	● very good stability in biological environments	● very good stability in biological environments ● 1 step synthesis and no purification
Cons for bioapplications	● lack of stability in biological environments ● hard to create large libraries of barcodes	● lack of monodispersity and size control ● long purification process	● technology doesn't allow yet to make monodisperse beads smaller than 4 μm

[a] Corresponding to QD barcodes synthesized according to the swelling approach.[18] [b] Corresponding to the QD barcodes synthesized according to the polymerization approach.[21]

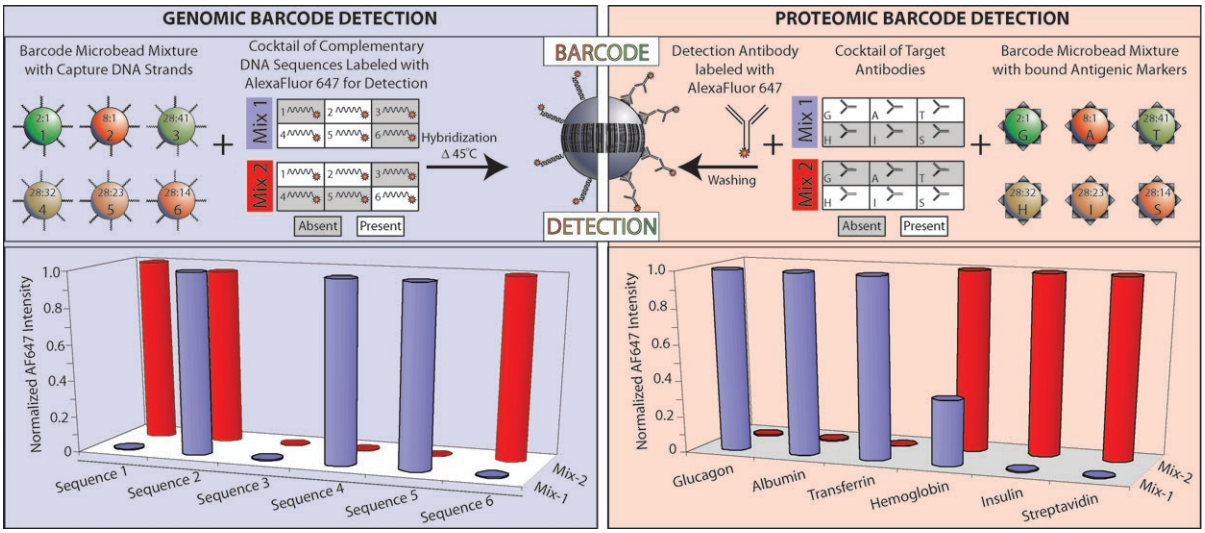

Figure 3. Multiplexed protein and DNA assays. Six DNA and six proteomic multiplexed assays were performed on the QD-barcoded beads. Triplicates were performed for each experiment and computed standard deviation was less than 10% in all cases.

embedded close to the surface of the microbead but homogeneously dispersed into the polymer matrix (see Figures S9 and S10 in the Supporting Information). This stability is absolutely essential to spectroscopic barcodes, and until now has been one of the major bottlenecks restricting further development toward commercialization and practical use. The use of this method to prepare QD barcodes solves issues surrounding the mass production, the encoding, and also the stability of QD barcodes, leaving only one last parameter to explore: surface bioconjugation and multiplexed assay detection.

Surface reactivity and multiplexing capabilities of the microbeads were tested on barcodes containing varying ratios of 520- and 580-nm emitting QDs. Specifically, we demonstrated barcoding ability with multiple targets by selecting six DNA sequences (ca. 30 base pairs) and six antigen–antibody–antibody sets in which the detection strand (genomic) or secondary antibody (proteomic) contains an AlexaFluor-647 (AF647) fluorescent dye marker. The same set of QD barcodes was used for both the DNA and antibody detection (Figure 3). Two separate mixes were made for DNA and protein analysis where certain detection strands or primary antibodies were added to the detection mix and others were not. In every case, all six barcodes were present. The bead samples were measured for green (QD-520, FL1 detector), orange (QD-580, FL2 detector), and red (AF647, FL4 detector) photoluminescence intensity by flow cytometry so that the ratio of green to orange intensities decodes each barcode, while AF647 intensity represents either the positive or negative presence of the sequence or antibody of interest. For example, Mix 1 contained sequences 2, 4, and 5 (genomic) or glucagon, albumin, and transferrin (G, A, and T; proteomic), and the red fluorescence intensities (FL4) are reported relative to a control in the absence of analyte after decoding the microbead barcodes. The results showed an average signal-to-noise ratio of 300; this result demonstrates that targeted detection is clearly visible above background fluorescence. All possible controls for nonspecific binding and cross-reactivity were performed for DNA and protein samples, (see Tables S1 and S2 in the Supporting Information), thus demonstrating that bioassay specificity is highly selective on barcode surfaces using our protocols.

Experimental Section

QD synthesis: ZnS-capped CdSe QDs were synthesized and characterized according to published procedures[29–31] and stored in chloroform.

CCFF barcoding process: Barcodes were prepared by mixing the QDs and poly(styrene-*co*-maleic anhydride) in chloroform. The resulting solution is then introduced into a nozzle system (Ingeniatrics) using a syringe pump (World Precision Instruments) at a rate of 1 mL h^{-1} along with the focusing fluid (water) using a digital gear pump (Cole Parmer Instruments) at a rate of 180 mL h^{-1}. The nozzle is then immersed in a water solution inside a modified ultrafiltration cell (Millipore 8000 series stirred system with 0.65-mm millipore mixed cellulose ester filter) under stirring. After synthesis, the valve is closed and barcodes are hardened by overnight stirring and then collected. A batch-to-batch reproducibility study was performed to demonstrate the robustness of the method (see Figure S11 in the Supporting Information). Microbead sizes can be tuned by adjusting the flow rates and the polymer concentration (see the Supporting Information).[32]

Optical images: Barcoded microbeads were placed onto a microscope slide and excited with a 100-W mercury lamp housed in an Olympus IX 71 fluorescence microscope. The signal was collected through a 40× objective (0.85 NA) and imaged with a color digital camera attached to the front port of the microscope.

Fluorescence spectra: Barcoded microbeads were placed onto a microscope slide and excited using a 488-nm Ar-ion laser line at 5 mW. The signal for a single QD barcode was collected by a 40× objective (0.85 NA), and a spectrum was obtained using a standard Acton spectrometer (with a grating of 150 grooves mm^{-1}) with a thermoelectrically cooled CCD camera placed on the side port of the microscope.[14] Integration time of the camera was set to 50 ms.

Other experimental details, including the detailed procedure for DNA and protein conjugation and multiplexing, can be found in the Supporting Information.

Received: January 25, 2008
Revised: March 20, 2008

Keywords: barcodes · biosensors · fluorescence · multiplexing · quantum dots

[1] N. J. Woodland, B. Silver, US patent 2,612,994, **1949**.
[2] N. H. Finkel, X. H. Lou, C. Y. Wang, L. He, *Anal. Chem.* **2004**, *76*, 353 A.
[3] R. Wilson, A. R. Cossins, D. G. Spiller, *Angew. Chem.* **2006**, *118*, 6250; *Angew. Chem. Int. Ed.* **2006**, *45*, 6104.
[4] F. Wang, W. B. Tan, Y. Zhang, X. P. Fan, M. Q. Wang, *Nanotechnology* **2006**, *17*, R1.
[5] B. D. Reiss, R. G. Freeman, I. D. Walton, S. M. Norton, P. C. Smith, W. G. Stonas, C. D. Keating, M. J. Natan, *J. Electroanal. Chem.* **2002**, *522*, 95.
[6] K. Braeckmans, S. C. De Smedt, C. Roelant, M. Leblans, R. Pauwels, J. Demeester, *Nat. Mater.* **2003**, *2*, 169.
[7] S. R. Nicewarner-Pena, R. G. Freeman, B. D. Reiss, L. He, D. J. Pena, I. D. Walton, R. Cromer, C. D. Keating, M. J. Natan, *Science* **2001**, *294*, 137.
[8] M. S. Gudiksen, L. J. Lauhon, J. Wang, D. C. Smith, C. M. Lieber, *Nature* **2002**, *415*, 617.
[9] S. Matthias, J. Schilling, K. Nielsch, F. Muller, R. B. Wehrspohn, U. Gosele, *Adv. Mater.* **2002**, *14*, 1618.
[10] F. Cunin, T. A. Schmedake, J. R. Link, Y. Y. Li, J. Koh, S. N. Bhatia, M. J. Sailor, *Nat. Mater.* **2002**, *1*, 39.
[11] D. C. Pregibon, M. Toner, P. S. Doyle, *Science* **2007**, *315*, 1393.
[12] H. X. Xu, M. Y. Sha, E. Y. Wong, J. Uphoff, Y. H. Xu, J. A. Treadway, A. Truong, E. O'Brien, S. Asquith, M. Stubbins, N. K. Spurr, E. H. Lai, W. Mahoney, *Nucleic Acids Res.* **2003**, *31*, 43e.
[13] M. Trau, B. J. Battersby, *Adv. Mater.* **2001**, *13*, 975.
[14] J. M. Klostranec, Q. Xiang, G. A. Farcas, J. A. Lee, A. Rhee, E. I. Lafferty, S. D. Perrault, K. C. Kain, W. C. W. Chan, *Nano Lett.* **2007**, *7*, 2812.
[15] H. Fenniri, S. Chun, L. H. Ding, Y. Zyrianov, K. Hallenga, *J. Am. Chem. Soc.* **2003**, *125*, 10546.
[16] P. Alivisatos, *Nat. Biotechnol.* **2004**, *22*, 47.
[17] V. Stsiapura, A. Sukhanova, M. Artemyev, M. Pluot, J. H. M. Cohen, A. V. Baranov, V. Oleinikov, I. Nabiev, *Anal. Biochem.* **2004**, *334*, 257.
[18] M. Y. Han, X. H. Gao, J. Z. Su, S. Nie, *Nat. Biotechnol.* **2001**, *19*, 631.
[19] D. Y. Wang, A. L. Rogach, F. Caruso, *Nano Lett.* **2002**, *2*, 857.
[20] X. H. Gao, S. M. Nie, *J. Phys. Chem. B* **2003**, *107*, 11575.
[21] P. O'Brien, S. S. Cummins, D. Darcy, A. Dearden, O. Masala, N. L. Pickett, S. Ryley, A. J. Sutherland, *Chem. Commun.* **2003**, 2532.
[22] W. C. Sheng, S. Kim, J. Lee, S. W. Kim, K. Jensen, M. G. Bawendi, *Langmuir* **2006**, *22*, 3782.
[23] M. Bradley, N. Bruno, B. Vincent, *Langmuir* **2005**, *21*, 2750.
[24] K. Boldt, O. T. Bruns, N. Gaponik, A. Eychmuller, *J. Phys. Chem. B* **2006**, *110*, 1959.
[25] J. A. Lee, A. Hung, S. Mardyani, A. Rhee, J. Klostranec, Y. Mu, D. Li, W. C. W. Chan, *Adv. Mater.* **2007**, *19*, 3113.
[26] A. M. Gañan-Calvo, *Phys. Rev. Lett.* **1998**, *80*, 285.
[27] A. M. Gañan-Calvo, J. M. Gordillo, *Phys. Rev. Lett.* **2001**, *87*, 4.
[28] Y. C. Cao, Z. L. Huang, T. C. Liu, H. Q. Wang, X. X. Zhu, Z. Wang, Y. D. Zhao, M. X. Liu, Q. M. Luo, *Anal. Biochem.* **2006**, *351*, 193.
[29] M. A. Hines, P. Guyot-Sionnest, *J. Phys. Chem.* **1996**, *100*, 468.
[30] B. O. Dabbousi, J. RodriguezViejo, F. V. Mikulec, J. R. Heine, H. Mattoussi, R. Ober, K. F. Jensen, M. G. Bawendi, *J. Phys. Chem. B* **1997**, *101*, 9463.
[31] X. G. Peng, M. C. Schlamp, A. V. Kadavanich, A. P. Alivisatos, *J. Am. Chem. Soc.* **1997**, *119*, 7019.
[32] L. Martín-Banderas, A. Rodriguez-Gil, A. Cebolla, S. Chavez, T. Berdun-Alvarez, J. M. F. Garcia, M. Flores-Mosquera, A. M. Ganan-Calvo, *Adv. Mater.* **2006**, *18*, 559.

